Int. J. Heat Mass Transfer. Vol. 34, No. 8, pp. 1975–1989, 1991
Printed in Great Britain

0017–9310/91 $3.00 + 0.00
Pergamon Press plc

Heat and mass transfer between a porous medium and a parallel external flow. Application to drying of capillary porous materials

W. MASMOUDI and M. PRAT†

Institut de Mécanique des Fluides, avenue du Professeur Camille Soula, 31400 Toulouse, France

(*Received* 13 *June* 1989 *and in final form* 25 *July* 1990)

Abstract—A numerical method allowing heat and mass transfer between an unsaturated porous medium and an external air flow to be predetermined is presented. Various numerical simulations are carried out in order to study the behaviour of the heat and mass convective transfer coefficients at the interface during drying. The simulations show that leading edge effects give rise to a space non-uniformity of the variables at the interface. It follows that the interfacial transfer coefficients differ from the standard values corresponding to boundary layer flows on the flat plate with uniform temperature or concentration at the wall. Furthermore, it is shown that one-dimensional simulation of the phenomena inevitably leads to incorrect results when the leading edge effects concern a sufficiently large part of the porous body. Lastly, the effect of the occurrence of large-scale heterogeneities of water content at the interface during drying is also studied.

1. INTRODUCTION

MANY PROCESSES involve heat and mass transfer between a porous medium and an external fluid. As an example of such processes directly connected with our study, one can quote the thermal insulation of buildings and the convective drying of porous materials. Two main reasons make the prediction of transfer difficult. The first is the great variety of configurations encountered in practice. Depending on the shape of the porous body, the determination of the external flow can be more or less difficult. Regarding transport properties, effective coefficients have to be determined for each porous medium.

The second reason is of fundamental nature. As it is well known and contrary to the external fluid, the practical modelling of the transfer in porous media is generally made at the so-called macroscopic level. The porous medium is then assimilated to a fictitious continuous medium and the variables of interest are not representative of transfer at the pore scale (the microscopic level) but of transfer at the scale of small volumes containing a sufficient number of pores. These volumes which are directly associated with the macroscopization process are called representative elementary volumes (REVs). For more details, one can refer to the presentation of Bachmat and Bear [1]. Consequently, the levels of description on the two sides of the interface between the porous medium and the external flow are different. Therefore, when we deal with a problem involving transfer both inside an external fluid and inside a porous medium, we must examine whether the levels of description of each medium are compatible.

As an example, we consider the problem sketched in Fig. 1. The external flow considered is a steady laminar flow at zero incidence (the case of fully turbulent flows is briefly commented on in the next section). The temperature, the specific humidity and the velocity of the incident external flow are denoted by T_∞, C_∞ and U_∞, respectively. The porous medium is assumed to be unsaturated, homogeneous and nondeformable. The initial moisture content and the initial temperature of the porous medium are assumed to be uniform and are denoted by ω_0 and T_0, respectively.

For such a situation, the traditional approach consists of first determining the external flow by assuming

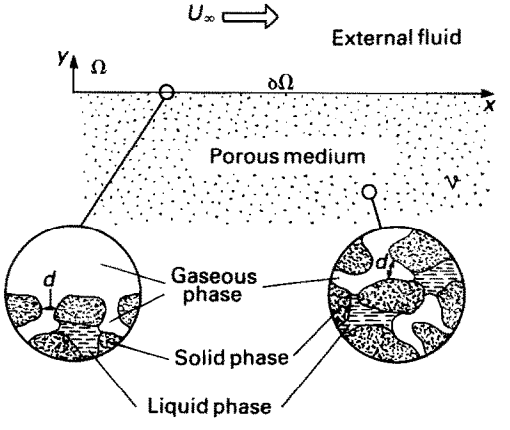

FIG. 1. Configuration studied.

† Author to whom correspondence should be addressed.

NOMENCLATURE

C specific humidity [kg kg^{-1}]
C_∞ specific humidity of the incident flow [kg kg^{-1}]
c_p heat capacity of the fluid phase [kcal kg^{-1} K^{-1}]
$(\rho c)^*$ mass fraction weighted heat capacity [kcal kg^{-1} K^{-1}]
$\mathscr{D}$ diffusion coefficient [m^2 s^{-1}]
D_m isothermal mass diffusivity coefficient [m^2 s^{-1}]
D_T non-isothermal mass diffusivity coefficient [m^2 s^{-1} K^{-1}]
D_v isothermal mass diffusivity coefficient in vapour phase [m^2 s^{-1}]
D_{vT} non-isothermal mass diffusivity coefficient in vapour phase [m^2 s^{-1} K^{-1}]
e evaporation flux density [kg m^{-2} s^{-1}]
g gravitational acceleration [m s^{-2}]
h local heat transfer coefficient [W m^{-2} s^{-1} K^{-1}]
$\bar{h}$ average heat transfer coefficient [W m^{-2} s^{-1} K^{-1}]
k local mass transfer coefficient [kg m^{-2} s^{-1}]
$\bar{k}$ average mass transfer coefficient [kg m^{-2} s^{-1}]
K hydraulic conductivity [m s^{-1}]
L macroscopic characteristic length [m]
$\mathscr{L}$ latent heat of vaporization [J kg^{-1}]
n outwardly directed unit normal vector
P pressure [Pa]
P_v water vapour partial pressure [Pa]
P_{vs} vapour saturation partial pressure [Pa]
Pr Prandtl number
q heat flux density at the interface [W m^{-2} s^{-1}]
R perfect gas constant [J kg^{-1} K^{-1}]
Re_x Reynolds number
Sc Schmidt number
t time [s]
T macroscopic temperature [K]
T_e external fluid temperature [K]
T_0 initial temperature [K]
T_∞ temperature of the incident flow [K]
U velocity [m s^{-1}]
U_∞ characteristic velocity of the external flow [m s^{-1}]
$\mathscr{V}$ volume of the porous medium domain [m^3]
x, y, z spatial coordinates.

Greek symbols
δ boundary layer thickness [m]
ζ unheated starting length [m]
λ_e external fluid thermal conductivity [kcal m^{-1} s^{-1} K^{-1}]
λ^* effective thermal conductivities [kcal m^{-1} s^{-1} K^{-1}]
ν kinematic viscosity of the fluid phase [m^2 s^{-1}]
ρ fluid phase density [kg m^{-3}]
ρ_e density of water [kg m^{-3}]
ρ_s density of dry material [kg m^{-3}]
ψ capillary potential [m]
ω mass moisture content [kg kg^{-1}]
ω_0 initial mass moisture content [kg kg^{-1}]
Ω volume of the external fluid phase [m^3]
$\partial\Omega$ dividing surface [m^2].

a no-slip condition at the porous surface. Afterwards, heat and mass transfer is obtained by coupling the equations describing transfers in both media by expressing the continuity of the temperature, the humidity in the gaseous phase, and the heat and mass normal flux densities at the interface.

Under these circumstances, the problem can be viewed as a classical problem of coupled transfer. However, comparison of experimental results to numerical simulation results based on this approach generally leads to some discrepancies [2]. In addition, the question of the heat and mass convective transfer coefficients at the interface is still unclear. Therefore, the main purpose of this paper is to provide some insights regarding these two problems.

The paper is organized as follows: in the first part, Sections 2 and 3, we try to identify as rigorously as possible the main approximations underlying the traditional approach. In the second part, Section 4, we examine, within the framework of the traditional approach, the consequences of the coupling of the transfers between the two media on the heat and mass transfer coefficients at the interface and on the procedure of comparison experience–simulation used in several studies of drying. Lastly, we discuss the discrepancies between numerical and experimental results which cannot be imputed to the coupling effect in the light of what we know of the approximations underlying the classic approach.

Clearly, as we are dealing with a convective transfer problem, we have first to address the question of the hydrodynamics of the system.

2. HYDRODYNAMICS OF THE SYSTEM

Obviously, the question of the hydrodynamics in such a system should be directly connected with the porous nature of the interface between the porous medium and the external flow. In fact, the hydrodynamics of the interfacial region has been the subject

of numerous studies. Most of them dealt with the problem of the determination of the relevant hydrodynamic conditions at the boundary of a porous medium domain [3–6] (for a more thorough literature survey, one can refer to the paper of Vignes-Adler *et al.* [7]). As far as we are concerned, we more especially refer to the work of Ene et Sanchez-Palencia [8] (see also Levy and Sanchez-Palencia [9]). When the typical length scales of the external flow are large compared with the microscopic scale (pore scale), they showed that the first approximation of the external flow can be obtained by imposing a no-slip condition. Actually, three zones should be distinguished from an asymptotic point of view (i.e. when the ratio of X to a typical size of pore d is very large or when the permeability tends to zero):

(a) An external zone, the structure of which is similar to a classic dynamic boundary layer.

(b) A zone inside the porous medium in which the Darcy law is valid.

(c) An intermediate layer which defines from the asymptotic point of view what we call the interfacial region and which has been studied by the method of matched asymptotic expansions by Ene and Sanchez-Palencia. They showed that its thickness is of the order of the pore scale and that the matching condition to be imposed in order to obtain the first approximation of the flow inside the porous medium is the continuity of the pressure.

More detailed information can be obtained by means of numerical computation of the microscopic flow within the interfacial region by considering model porous media [6, 10]. These simulations lead basically to the same results as those of Ene and Sanchez-Palencia [8]; i.e. for the asymptotic situation, extra convective effects exist in a very thin region of the order of d at the interface and the no-slip condition is appropriate to determine the external flow.

The extra flow in the porous medium at the interfacial region is mainly due to the shear at the interface. However, for reasonable Schmidt or Prandtl numbers as here in the case of an air flow, it can be shown that this extra flow can be neglected regarding the heat and mass transfer for the asymptotic situation.

Finally, from the asymptotic point of view, the determination of the flow inside both media consists in first calculating the external flow by imposing a no-slip condition at the interface (the porous body is then viewed as impervious). Afterwards, the flow inside the porous medium is computed by imposing at the interface the pressure distribution deduced from the external flow determination.

As an example, the situation illustrated in Fig. 2 has been computed. The first approximation of the external flow is a boundary layer flow on a flat plate. As is well known for such a flow, the pressure of the outer flow is impressed at the wall. Due to this longitudinal pressure gradient, a macroscopic flow takes place in the porous medium. It is the result of

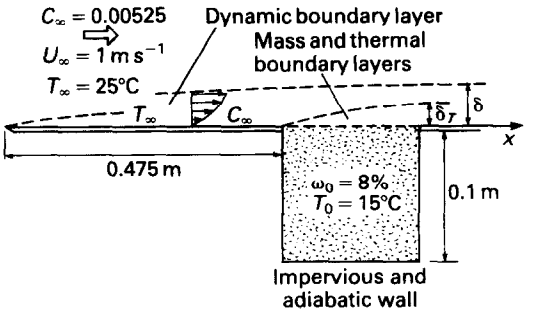

FIG. 2. Configuration numerically studied.

the macroscopic dynamic coupling between the two media. However, taking into account the values of the longitudinal pressure gradient existing in such a type of external flow and the values of air permeabilities of most of the unsaturated porous material of interest, it is easy to check that the so-induced filtration flow has generally very little influence on the heat and mass transfer for the configuration considered. Therefore, in the following, the gas phase pressure in the porous body will be considered as uniform and constant. Also, one can note regarding the condition at the interface for the external flow that a blowing effect due to evaporation must be, in principle, taken into account. However, in the case of drying at relatively low temperature that we consider here such an effect can be ignored.

Lastly before concluding this hydrodynamic part, we have to briefly examine the case of an external turbulent flow. Turbulent external flows are in fact rather the rule than the exception. In this case however, we cannot expect a solid theoretical analysis similar, for instance, to the one made by Ene and Sanchez-Palencia [8] for the laminar case. Therefore, we only want to give in the following some 'plausible' arguments leading eventually to the same kind of modelling as for the laminar case. First of all, as the typical time scales of the turbulence are generally much smaller than the characteristic time scale of the transfer between the porous body and the external flow it seems quite reasonable to couple the macroscopic equations of the porous body with the time averaged equations of continuity, momentum and energy for the external fluid. However, as density variations due to temperature and specific humidity variations take place in the fluid, a treatment for variable density flow should be, in principle, considered [11]. In fact, for situations of moderate transfer, the variations of density may be ignored and one can rely on a classical incompressible flow treatment [12]. For the situation sketched in Fig. 2, various turbulence models (mixing length, k–ε with or without wall functions ...) lead to a sufficiently good determination of the heat and mass flux densities at the interface [13]. Under these circumstances, the problem formally takes the same form as for the laminar case.

If one is only interested in determining the transfer at the interface and inside the porous body, a procedure basically similar to that carried out for the laminar case may be used, see Section 4.

However, it should be noted that such a procedure is based in fact on the assumption that turbulence along a porous interface does not significantly differ from turbulence along a classical flat plate. Such an assumption seems reasonable from the asymptotic point of view, that is to say when the typical space scale of the pores at the interface is notably smaller than the typical scale of the characteristic eddies in the near wall region, see Grass [14] and Kline [15] among others (for the kind of flow considered in this study, this typical scale is of the order of 1 mm, that is to say relatively large compared with the pore size of the traditional porous media). Nevertheless, taking into account the porous nature of the interface, the above-mentioned near wall structures could not be exactly the same as those observed along classical flat plates.

In this connection, an increase of the cross-stream fluctuating velocity at a porous interface is expected, see Liu and Mount [16] among others. Therefore, performances of the standard models of turbulence should be carefully examined for the case of such interfaces.

From the point of view of transport phenomena in porous media, the existence of various fluctuating fields (pressure, velocity, temperature, humidity) at the interface could influence transfers in the interfacial region. Under these circumstances, it could be necessary to re-examine the modelling.

We stop, here, the list of such open problems and simply assume that the above-mentioned effects are of negligible influence when the pore size is sufficiently small compared with the typical scales of turbulence. As stated above, the procedure is then similar to that for the laminar case.

To conclude this section, it seems that the approximations more or less implicitly made within the framework of the traditional approach are very reasonable as far as the fluid dynamics is concerned when the typical size of the pore is sufficiently small relative to the characteristic scales of the external flow. In other words, possible weaknesses of the traditional approach do not seem to be a priori associated with the problem of the dynamics of the interfacial region.

3. HEAT AND MASS TRANSFER MODELLING

Coupled heat and mass transfer in unsaturated capillary porous media has been the subject of many studies. One can refer to Crausse [17], Moyne [18] or Bories [19] for a literature survey. As we have said before, the operational modelling of transfer phenomena in porous media is generally made at a macroscopic level allowing us to view the porous medium as a fictitious continuum. In the case of heat and mass transfer in unsaturated capillary porous media, the basic equations at the macroscopic level were established by Philip and de Vries [20] and approximately at the same time by Luikov [21]. These equations can be written as

$$\frac{\partial \omega}{\partial t} = \nabla \cdot (D_\omega \nabla \omega + D_T \nabla T) - \nabla \cdot \left(\frac{\rho_e}{\rho_s} K \nabla y \right) \quad \text{in } \mathcal{V} \tag{1}$$

$$(\rho c)^* \frac{\partial T}{\partial t} = \nabla \cdot ((\lambda^* + \mathscr{L} \rho_s D_{vT}) \nabla T + \mathscr{L} \rho_s D_v \nabla \omega) \quad \text{in } \mathcal{V} \tag{2}$$

in which ω and T denote the local mass moisture content and the local temperature in the porous medium domain $\mathcal{V}$, respectively. All coefficients of equations (1) and (2) are dependent variables of moisture content and temperature and must be specifically determined for each porous medium, see Crausse [17] for more details.

To our knowledge, these equations have not yet been derived from the microscopic equations by means of a rational approach such as for instance the volume averaging method [22] in a completely satisfactory way. Doubt remains with regard to the validity of these equations from a theoretical point of view. Indeed, mass transfer within the porous medium can be viewed here as an unsteady two-phase flow process. It has been shown (see for instance Lenormand *et al.* [23]) that one cannot expect to describe certain two-phase flow processes in porous media according to a continuum approach because of the occurrence of large-scale heterogeneities in the fluid distribution within the medium. These heterogeneities are associated with the action of the capillary forces in a system containing a sufficient distribution of pore size. In some cases, moisture content heterogeneities could also be associated with macroscopic heterogeneities of the structure [24].

However, in the case of drying, experiments carried out with micromodels [25, 26] as well as the experiments of Shaw [27] with random packing of silica spheres show that the heterogeneities are of limited size and that this size is relatively constant during most of the process. In other words, it seems to be possible to rely on a continuum approach. However, the size of the REV should be considered as controlled by the size of the moisture content heterogeneities and therefore should be viewed as quite large relative to a typical size of pore or grain (fingering of the order of 600 particle size has been observed by Shaw [27]!). Consequently, according to this analysis, small values of the ratio of the pore size to the characteristic length scales of the external flow do not guarantee that we are dealing with an asymptotic situation in terms of the heat and mass transfer coupling. In principle, we need in fact a small ratio of the size of the moisture content heterogeneity (or of the size of an REV) to the external flow length scales in order to couple the equations according to the traditional approach.

In this connection, it may be useful to place our study with respect to the works of Suzuki and Maeda [28] and Schlunder [29] in which they study the influence of the discontinuous character of the vapour sources at the interface, see Fig. 3, upon the mass transfer between the porous medium and the external flow. It should be emphasized that their studies have nothing to do with the moisture content heterogeneities described above and also, that the problem they consider is of no interest here when the pore size is sufficiently small with respect to the external flow length scale.

To summarize this part, the traditional approach seems to hold when the size of the moisture content heterogeneities associated with the action of the capillary forces are small enough. Clearly, this constraint is much more severe than the constraint associated with an asymptotic behaviour for the dynamics, Section 2, and is probably not satisfied in many situations of interest. However, it should be noted that the large-scale heterogeneities of moisture content during drying have been only observed so far for initially saturated porous media. Further studies are in order for intermediate initial saturation states. For the configuration studied here, the classic approach takes the form:

External flow

$$\nabla \cdot U = 0 \quad \text{in } \Omega \tag{3}$$

$$U \cdot \nabla U = -\frac{1}{\rho}\nabla P + \nu \frac{\partial^2 U}{\partial y^2} \quad \text{in } \Omega \tag{4}$$

$$U \cdot \nabla T_e = \left(\frac{\lambda_g}{\rho c_p}\right)\frac{\partial^2 T_e}{\partial y^2} \quad \text{in } \Omega \tag{5}$$

$$U \cdot \nabla C = \mathscr{D}\frac{\partial^2 C}{\partial y^2} \quad \text{in } \Omega. \tag{6}$$

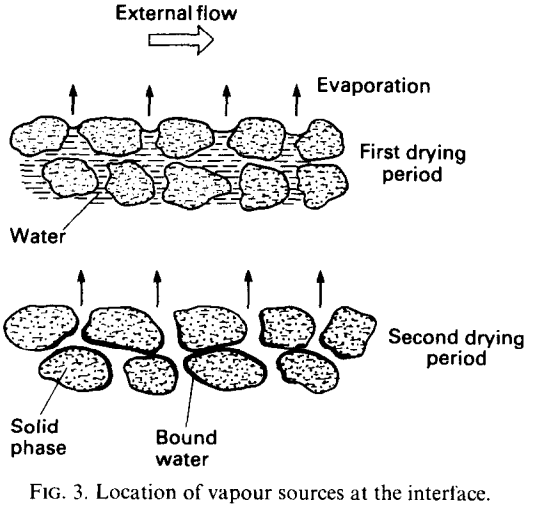

FIG. 3. Location of vapour sources at the interface.

Porous medium

$$\frac{\partial \omega}{\partial t} = \nabla \cdot (D_\omega \nabla \omega + D_T \nabla T) - \nabla \cdot \left(\frac{\rho_e}{\rho_s} K \nabla y\right) \quad \text{in } \mathscr{V} \tag{7}$$

$$(\rho c)^* \frac{\partial T}{\partial t} = \nabla \cdot ((\lambda^* + \mathscr{L}\rho_s D_{vT})\nabla T + \mathscr{L}\rho_s D_v \nabla \omega) \quad \text{in } \mathscr{V}. \tag{8}$$

Boundary conditions at the interface

Continuity of the state variables

$$U = 0 \quad \text{at } \partial\Omega \tag{9}$$

$$T_e(x,0) = T(x,0) \quad \text{at } \partial\Omega \tag{10}$$

$$C(x,0) = \frac{P_v M_e}{M_a(P - P_v) + M_e P_v} \quad \text{at } \partial\Omega \tag{11}$$

in which $P_v = P_{vs} \exp(gM_e\psi/RT(x,0))$, Kelvin's relation.

Continuity of the flux densities

$$(\lambda^* + \mathscr{L}\rho_s D_{vT})\nabla T \cdot n_y + \mathscr{L}\rho_s D_v \nabla \omega \cdot n_y = \lambda_g \nabla T_e \cdot n_y + \mathscr{L}\rho\mathscr{D}\nabla C \cdot n_y \quad \text{at } \partial\Omega \tag{12}$$

$$\rho_s D_\omega \nabla \omega \cdot n_y + \rho_s D_T \nabla T \cdot n_y - \rho_e K = \rho\mathscr{D}\nabla C \cdot n_y \quad \text{at } \partial\Omega. \tag{13}$$

Together with the above relations, boundary conditions at the other boundaries of domains Ω and $\mathscr{V}$ must be specified.

No time derivative appears in equations (4)–(6). Indeed, one can show that the characteristic time scales of the external flow are much smaller than the time scales of the transfers inside the porous body. The time evolution for the external flow can thus be viewed as a succession of steady states.

Thus, the problem takes the form of a classical conjugate transfer problem with the following important differences:

(a) We are essentially interested in the transient phase of the process.

(b) The coefficients that appear in equations (7) and (8) vary by several orders of magnitude as a function of the moisture content [2]. Therefore, we deal with non-linear equations.

These points distinguish our study from the previous works of Sifaoui and Perrier [30] and Morgan and Yerazunis [31] in which they considered various steady state evaporation regimes.

Due to the non-linear character of equations (7) and (8), a numerical procedure should be carried out in order to solve the set of equations (3)–(13). The procedure is briefly presented in the next section.

4. A NUMERICAL STUDY

One can carry out a numerical procedure allowing the solution of equations at each time step both in the porous body and in the external flow [32]. However, if one is mainly interested in determining transfers at the interface and inside the porous body, the use of local heat and mass convective coefficients at the interface considerably simplifies the procedure. Assuming low specific humidity (drying at relatively low temperature), such coefficients denoted by $h(x)$ and $k(x)$, respectively, are defined by

$$h(x) = \frac{q(x)}{(T(x,0) - T_e)} \tag{14}$$

$$k(x) = \frac{e(x)}{(C(x,0) - C_e)} \tag{15}$$

in which $q(x)$ and $e(x)$ represent the heat flux densities and the mass flux densities at the interface, respectively.

These coefficients are not intrinsic properties of the flow. In particular, their values depend on the temperature and specific humidity distributions at the interface. The non-uniformity of the temperature and of the specific humidity at the interface during the drying process can be taken into account by means of the superposition method [33]. Equations (7) and (8) have been solved by means of a finite element method, see ref. [34] for more details.

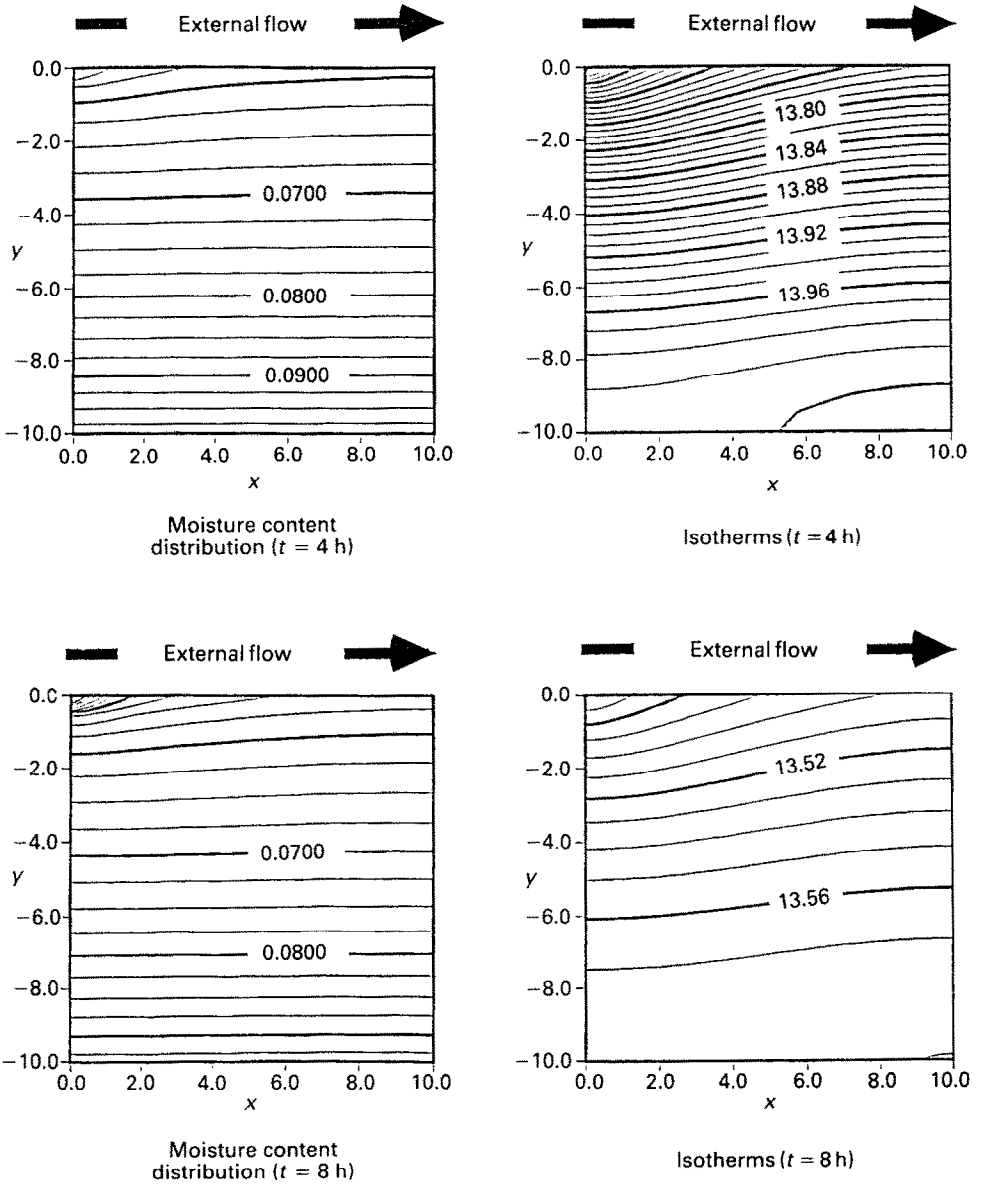

FIG. 4. Isotherms and moisture content distribution inside the porous body at various times (initial moisture content of 8%).

In the following, numerical simulations are used to study the behaviour of the convective coefficients at the interface. We successively consider a material in the first drying period (constant drying rate, moisture content values at every point of the interface are above the maximum sorption moisture) and in the second drying period (falling drying rate period, the moisture content at some or all points of the interface is below the maximum sorption moisture). We first present the main results of the simulation for the configuration sketched in Fig. 2. A laminar external flow is assumed. The temperature, the specific humidity and the velocity of the incident flow are given in Fig. 2.

4.1. *Main simulation results*

4.1.1. *First drying period.* The simulation is carried out for an initial moisture content of 8%. Figure 4 shows the space and time evolution of the moisture content and temperature fields inside the porous body. The thermal and mass boundary leading edge effect is clearly shown. This effect is linked to the high mass and thermal flux densities in the leading edge region as can be seen in Fig. 5 in which the distributions of the moisture content and the temperature at the interface are also shown. Here, evaporation occurs at the interface. Mass transfer in the porous medium towards the interface is mainly due to capillary flow of the liquid phase (one can refer to Bories [19] or Bories *et al.* [35] for more details regarding the moisture transport mechanisms).

4.1.2. *Second drying period.* For the same characteristics of the external flow as previously, an initial moisture content of 3% is considered. The computed moisture and temperature fields are shown in Fig. 6. One can notice the occurrence of a dry or sorption zone linked to the recession of the evaporation front. The main mechanism of moisture transport in the dry zone is vapour transport [19, 35]. In the case of the

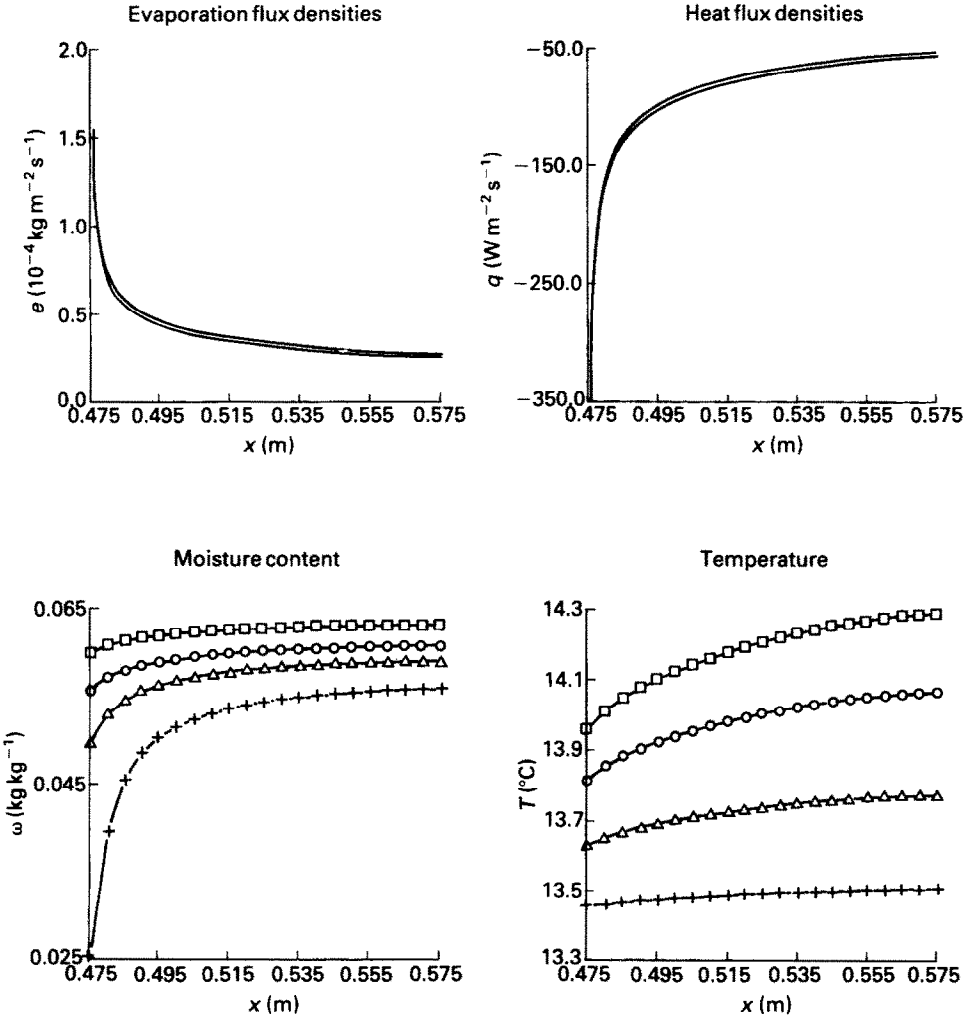

FIG. 5. Space evolution of the temperature, the moisture content and the heat and mass flux densities at the interface at various times (initial moisture content of 8%): □-□-□, 1 h; ○-○-○, 2 h; △-△-△, 3 h; +-+-+, 4 h.

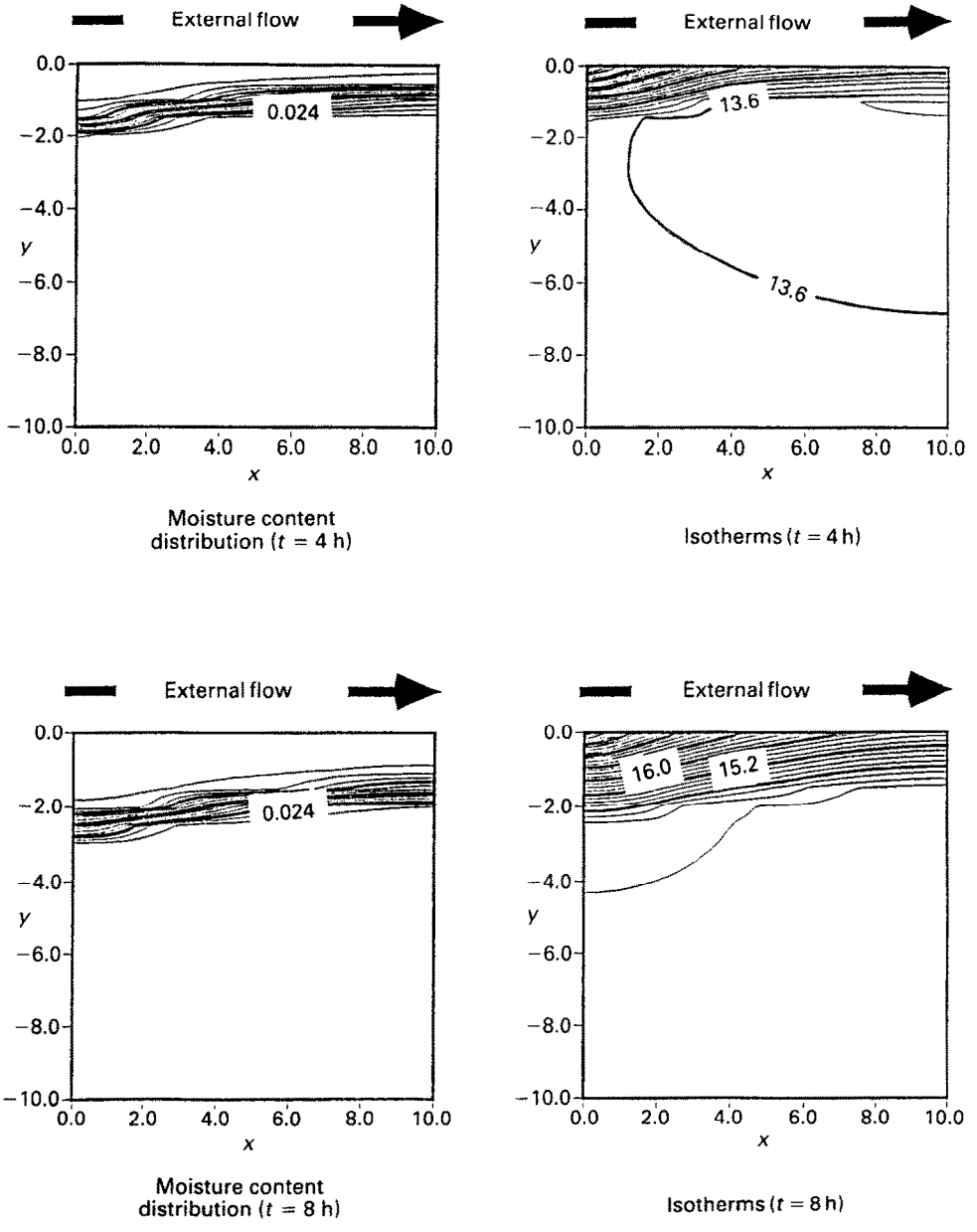

FIG. 6. Isotherms and moisture content distribution inside the porous body at various times (initial moisture content of 3%).

sorption region, movement of the bound water is also invoked [36]. Here again, one can notice in Fig. 6 the thermal and mass boundary layer leading edge effect. Space and time evolutions of the mass and thermal flux densities at the interface can be seen in Fig. 7.

4.2. *Heat and mass transfer analogy at the interface*

In many situations, the equations describing the mass transfer and the heat transfer in the external flow take an analogous form, see for instance equations (5) and (6). Therefore, if the boundary conditions take also the same form, one can deduce solutions concerning one of the transfers from the solution concerning the other one. For instance, one can deduce the values of the local mass convective transfer coefficient from the values of the local heat transfer coefficient. For a boundary layer flow on a flat plate, the ratio of the local mass transfer coefficient to the local heat transfer coefficient has a value of about 10^{-3} U.S.I. [33]. Here, such an analogy should be valid during the first period of drying since the specific humidity at the interface depends only on the interfacial temperature. This point has been recently investigated by Perrin and Darolles [37]. After some corrections [34], the experimental results fairly confirm the validity of the analogy.

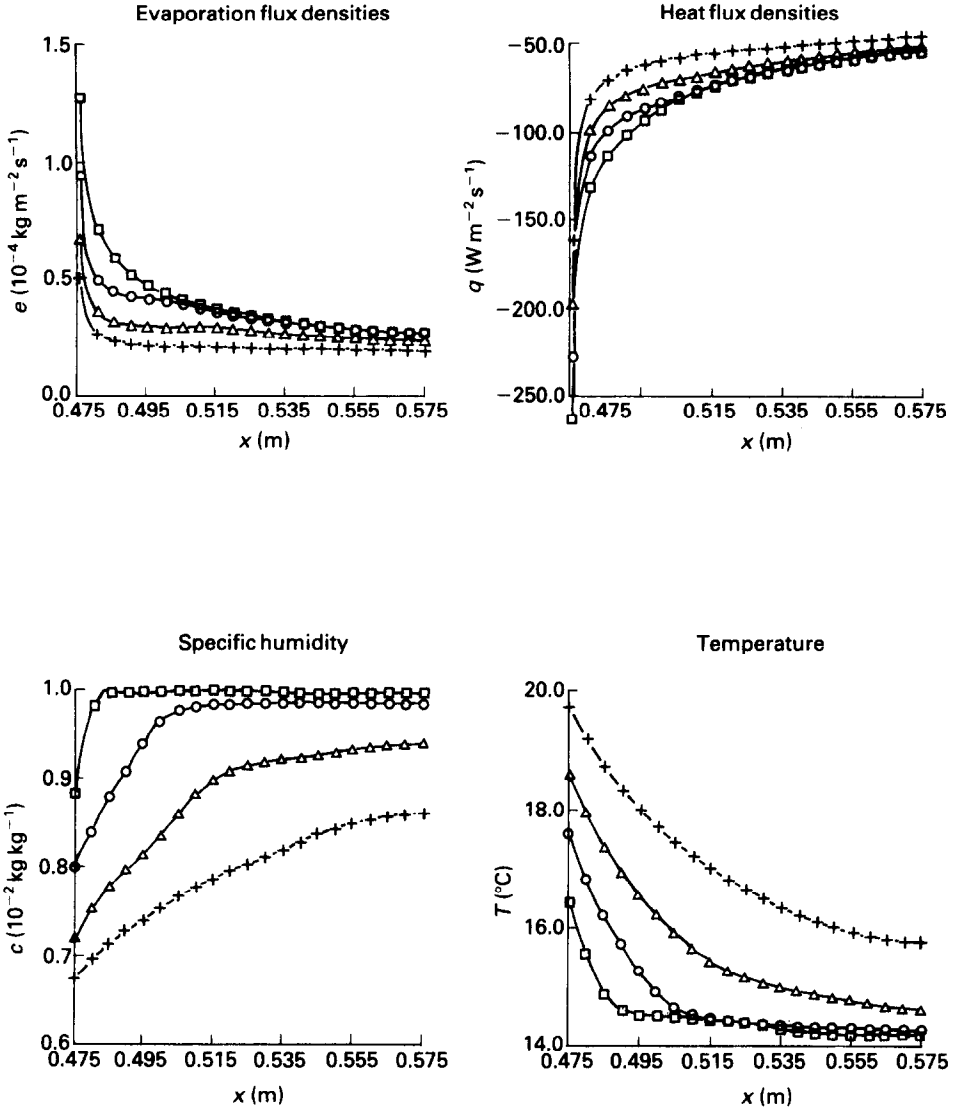

FIG. 7. Space evolution of the temperature, the moisture content and the heat and mass flux densities at the interface at various times (initial moisture content of 3%): □-□-□, 1 h; ○-○-○, 2 h; △-△-△, 3 h; +-+-+, 4 h.

During the second period of drying, sorption mechanisms at the interface should be taken into account. The specific humidity at the interface depends not only on the temperature but also on the moisture content at the interface. Therefore, the boundary condition at the interface for heat transfer may be different from the boundary condition for the mass transfer. However, the results drawn from our simulation [34] do not show a dramatic discrepancy between the calculated ratio and the standard value of 10^{-3} U.S.I. Nevertheless, noticeable discrepancies may be expected for other drying conditions.

4.3. *Heat and mass convective transfer coefficients at the interface*

The 'standard' or reference values of the transfer coefficients correspond to the case of a thermal and mass boundary layer on a flat plate with a starting length. The temperature or the specific humidity is assumed to be equal to the temperature or the specific humidity of the incident air flow for x smaller than ζ (Fig. 8). For $x > \zeta$, a uniform temperature or humidity is assumed. Under these circumstances, the coefficients can be expressed as

$$k(x) = C1 \frac{\rho \mathscr{D}}{x} Sc^p (U_\infty x/\nu)^m (1 - (\zeta/x)^n)^{-q} \quad (16)$$

$$h(x) = C1 \frac{\lambda_g}{x} Pr^p (U_\infty x/\nu)^m (1 - (\zeta/x)^n)^{-q} \quad (17)$$

in which the values of $C1$ and of the various exponents depend on the nature of the flow (for a laminar flow, $C1 = 0.332$, $p = 1/3$, $m = 1/2$, $n = 3/4$, $q = 1/3$).

As can be seen in Figs. 4 and 6 or 5 and 7, the

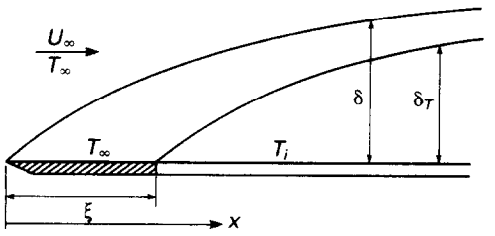

FIG. 8. Boundary layer development on a plate with an unheated starting length.

temperature and the specific humidity at the interface are not uniform during the process. Therefore, the effective values of the convective coefficients at the interface may differ from the standard values given by equations (16) and (17). Furthermore, the time evolution of the temperature and humidity distribution at the interface during drying (see Fig. 5 or 7) induces a time evolution of the convective coefficient values. However, in our simulations, the obtained variations with respect to the standard values are of the order of 10% or less. These variations should be a priori completely distinguished from the variations with the moisture content considered for instance by Suzuki and Maeda [28], Van Brakel and Heertjes [38] or Chen and Pei [36].

As we stated above, the variations with respect to the standard values that we obtained should be attributed to the non-uniform distribution of the temperature and the moisture content at the interface during the process. As regards the variations considered by Chen and Pei [36], wet area fraction variations at the interface during drying are invoked. In terms of order of magnitude, they consider huge variations of the convective coefficients with moisture content (for instance variation of 90% of the initial value of the coefficient is considered).

According to the asymptotic point of view, it seems difficult to give theoretical foundation to such variations of the coefficient with moisture content. Although an attempt at an explanation based on large-scale heterogeneities of the water content at the interface is considered in Section 4.3, we give below a completely different interpretation of the necessity of considering variation of the coefficient when the predetermination of the transfers is carried out by means of a one-dimensional simulation as Chen and Pei did.

4.4. *Consequences of the simulation of the phenomena by means of one-dimensional simulations*

As for the experiments mentioned by Chen and Pei [36], various authors have considered convective drying situations similar to the one sketched in Fig. 3. One can quote the works of Crausse [17], Sifaoui and Perrier [30], Morgan and Yerazunis [31], Perrin and Darolles [37], Gidas and Constantinou [39], Bories *et al.* [35] among others. Generally, the validity of the proposed mathematical model of drying is argued after comparing experimental results with numerical results obtained by one-dimensional simulation. In the following, we show that such a procedure cannot generally lead to a relevant comparison between numerical results and experimental ones because a one-dimensional simulation inevitably ignores the thermal and mass boundary layer leading edge effect exhibited in Section 4.1.

In the following, some results drawn from the two-dimensional simulations for the initial moisture content of 3%, see Section 4.1, are henceforth viewed as 'experimental results'. The considered 'experimental' results correspond to those classically obtained in the real experiments like those presented in some of the above-mentioned references. That is to say, the vertical profiles of temperature and moisture content in the middle of the cell at various times (sometimes, vertical slice average moisture content profiles are also

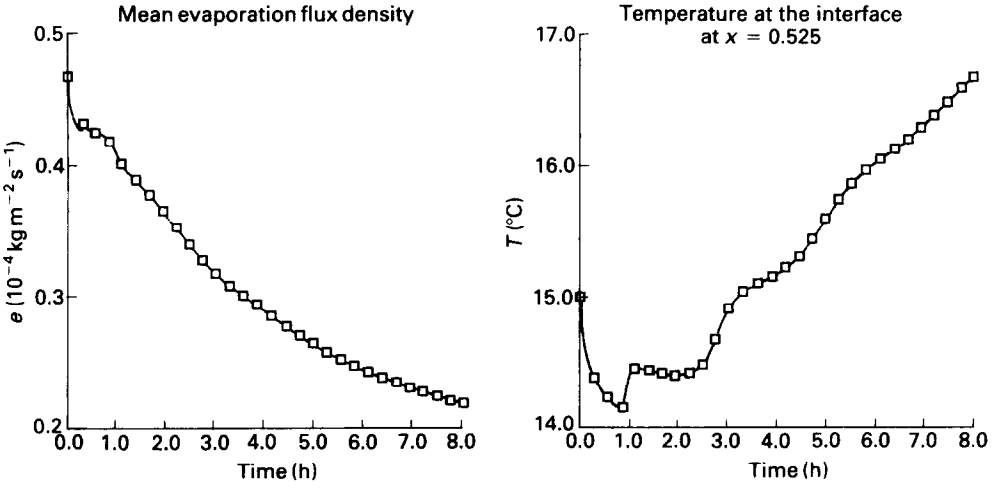

FIG. 9. Evolution of the average evaporation flux density and the interfacial temperature at $x = 0.525$ obtained by two-dimensional simulation (initial moisture content of 3%).

considered [17]); the time evolution of the temperature at a point of the interface (here we consider the temperature at $x = 0.525$, see Fig. 9); the evaporation law (time evolution of the average evaporation flux density at the interface).

Let us suppose that we want to simulate these 'experimental results' by means of a one-dimensional simulation. Several possibilities may be considered as regards the boundary conditions at the interface. Some of the most obvious possibilities are summarized in Table 1.

In Table 1, $\bar{h}$ and $\bar{k}$ represent the standard average heat transfer coefficient and the standard average mass transfer coefficient at the interface, respectively

$$\bar{h} = \frac{1}{L}\int_{\zeta}^{\zeta+L} h(x)\,\mathrm{d}x \tag{18}$$

$$\bar{k} = \frac{1}{L}\int_{\zeta}^{\zeta+L} k(x)\,\mathrm{d}x. \tag{19}$$

Table 1. Some of the possible upper boundary conditions for a one-dimensional simulation

Case no.	Thermal boundary condition	Mass boundary condition
1	$\bar{h}$	$\bar{k}$
2	$h(0.525)$	$k(0.525)$
3	$h(0.525)$	mean evaporation flux density 'measured'
4	$\bar{h}$	mean evaporation flux density 'measured'
5	'measured' temperature at $x = 0.525$	$k(0.525)$
6	'measured' temperature at $x = 0.525$	mean evaporation flux density 'measured'

The various results obtained by means of one-dimensional simulations are compared with the 'experimental' results (two-dimensional simulation) in Fig. 10. As can be seen in the figure, one cannot expect to

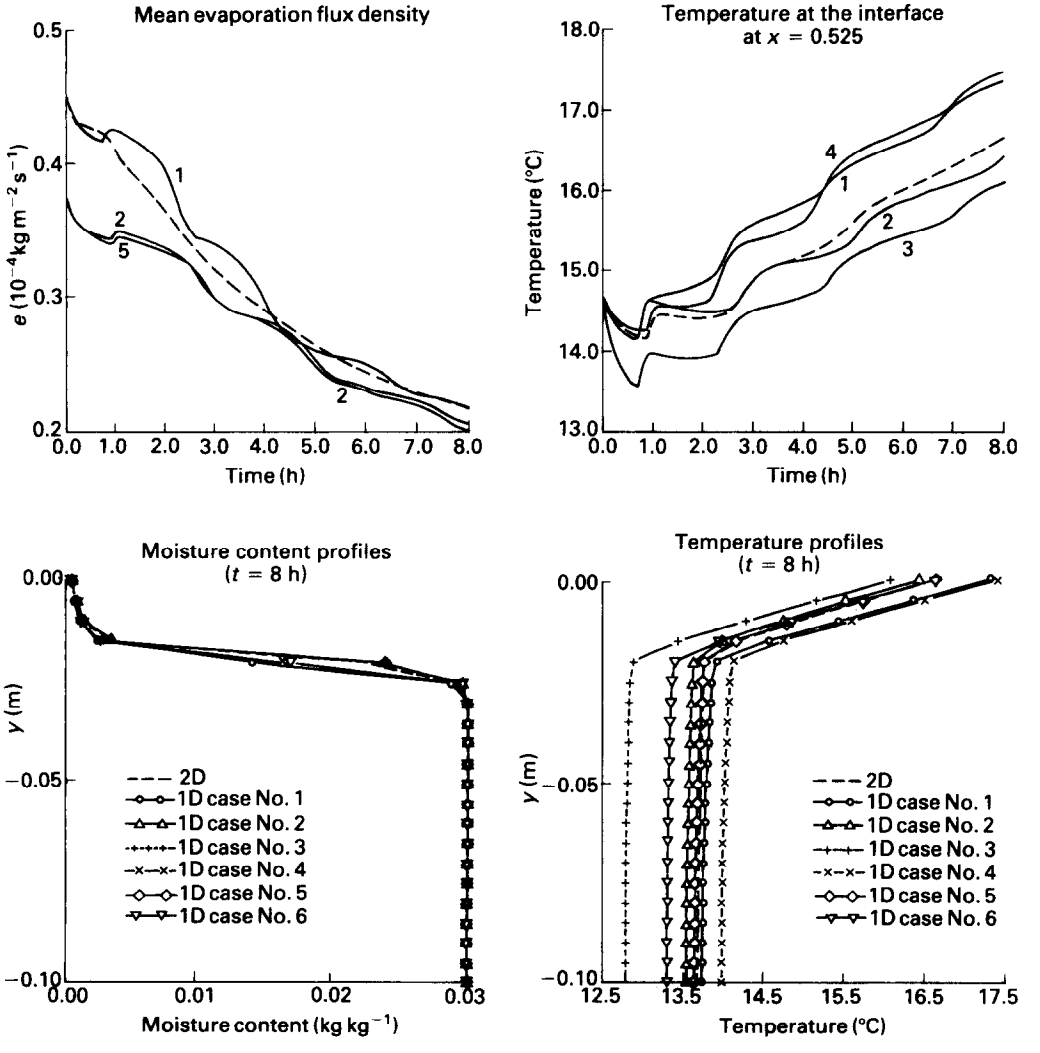

FIG. 10. Comparison between results of one- and two-dimensional simulations (mentioned numbers refer to Table 1).

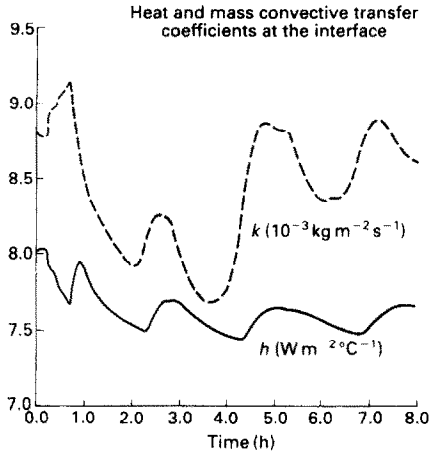

FIG. 11. Heat and mass convective transfer coefficients that we would have to consider in order to correctly compute the 'experimental' average heat and mass flux densities by means of one-dimensional simulation.

realistically reproduce the experimental results by means of one-dimensional simulations.

Of course, the convective coefficients at the interface can be more or less adjusted in order to reproduce the experimental results. As an example, Fig. 11 shows the time evolution of the heat and mass transfer coefficients that we would have to consider in order to correctly simulate the evaporation law and the 'experimental' average heat flux density at the interface by means of a one-dimensional computation. Appreciable variations of the coefficients are obtained. Taking into account these results, it seems to us that the correct procedure of validation consists in comparing experimental results and two-dimensional simulation (or three-dimensional simulation if it is necessary!) results without an adjustable parameter. Clearly, in order to correctly carry out such a procedure, a precise characterization of the external flow should be made.

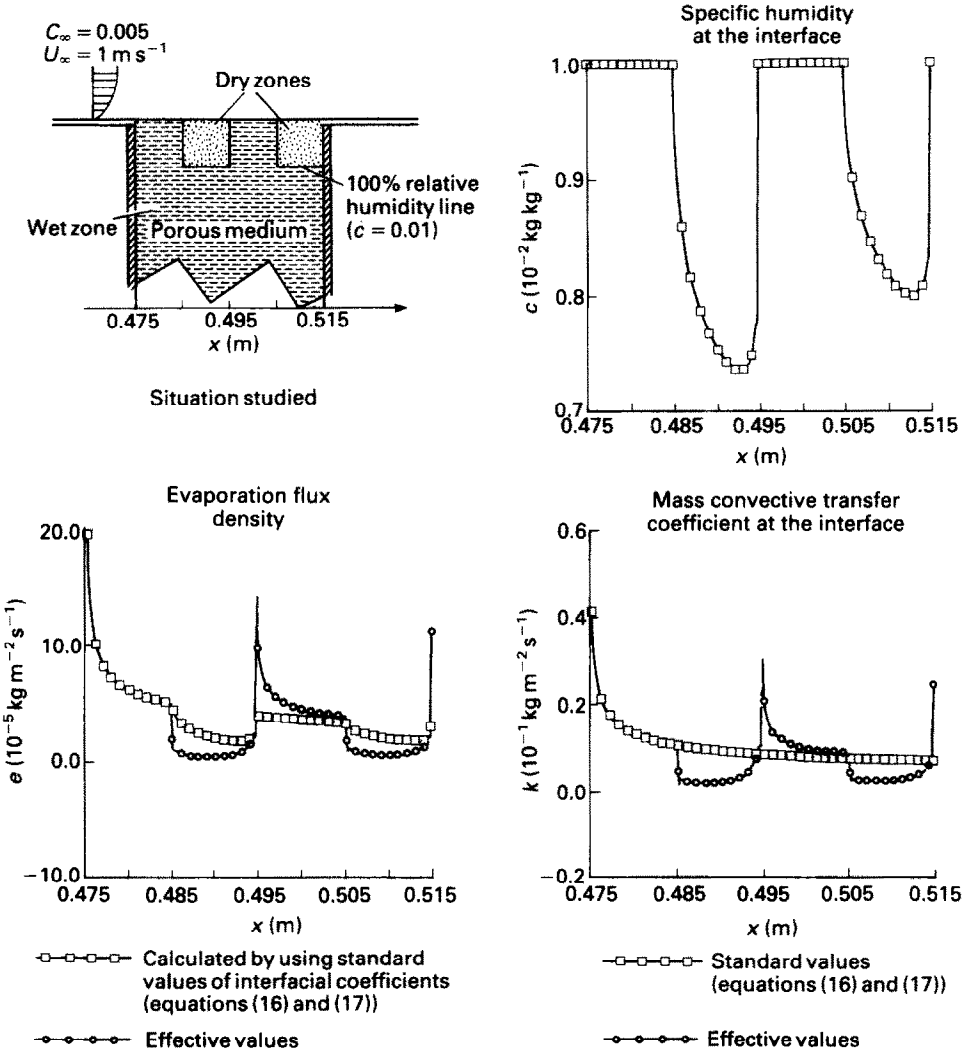

FIG. 12. Influence of macroscopic heterogeneities of moisture content at the interface upon the local mass convective transfer coefficient.

4.5. *Effect of macroscopic heterogeneities of moisture content during drying*

So far, we have assumed the asymptotic point of view holds. That is to say the size of the REV is small enough. However, taking into account the size of the moisture content heterogeneities observed for instance by Shaw [27] (of the order of 600 grains, see Section 3), one can in fact suspect that large-scale heterogeneities of moisture content generally exist in the interfacial region.

In order to estimate the influence of such moisture content heterogeneities upon the mass transfer coefficients at the interface, the moisture content distribution at the interface sketched in Fig. 12 has been considered. For the same characteristics of the external flow as previously, the mass transfer for such a moisture content distribution has been computed by performing the same kind of simulation as in the previous sections. The main results are given in Fig. 12. In particular, Fig. 12 shows the influence of such heterogeneities upon the local mass transfer coefficient. As regards the average mass flux density at the interface, the use of the standard coefficient leads, here, to an overestimate of about 10%.

5. CONCLUSION

The approximations underlying the traditional modelling of the drying of capillary porous material have been investigated. It has been shown that such an approach is based on a double asymptotic point of view. When the ratio of the typical size of the pore to the characteristic scales of the external flow is small enough (first asymptotic point of view), the particular dynamic effects taking place in the interfacial region can be ignored. This length scale constraint seems to be commonly encountered in practice. When the ratio of the typical size of the moisture content heterogeneities to the characteristic external flow length scales is small enough (second asymptotic point of view), standard coupling of the macroscopic equations describing transfers inside the porous medium with the equations describing transfers in the external flow is probably valid. When this double asymptotic point of view holds, two-dimensional numerical simulations have clearly exhibited the influence of the thermal and mass boundary layer edge effect. It follows that the correct procedure of model validation necessarily involves two-dimensional (or possibly three-dimensional) simulation when the area of the interface is not significantly large with respect to the mass or thermal boundary leading edge zones. In this connection, it should be noted that a turbulent flow presents leading edge zones smaller than the corresponding laminar one. Under these circumstances, the use of variable heat and mass transfer coefficients together with one-dimensional simulation seems to be an artefact.

However, taking into account the size of the large-scale moisture content heterogeneities one can expect in practice, the transfer at the interface could be strongly affected by the existence of such heterogeneities as numerical simulations show. Clearly, careful investigations of the phenomena taking place inside the porous material are still needed.

Acknowledgement—Financial support from PIRSEM–CNRS is gratefully acknowledged.

REFERENCES

1. Y. Bachmat and J. Bear, Macroscopic modelling of transport phenomena in porous media. 1: The continuum approach, *Transport Porous Media* **1,** 213–240 (1986).
2. P. Crausse, G. Bacon et S. Bories, Etude fondamentale des transferts couplés chaleur-masse en milieu poreux, *Int. J. Heat Mass Transfer* **24,** 991–1004 (1981).
3. G. S. Beavers and D. D. Joseph, Boundary conditions at a naturally permeable wall, *J. Fluid Mech.* **30**(1), 197–207 (1967).
4. P. G. Saffman, On the boundary condition at the surface of a porous medium, *Studies Appl. Math.* **L**(2), 93–101 (1971).
5. S. M. Ross, Theoretical model of the boundary condition at a fluid porous interface, *A.I.Ch.E. Jl* **29,** 840 (1983).
6. R. E. Larson and J. J. L. Higdon, Microscopic flow near the surface of two-dimensional porous media, *J. Fluid Mech.* **166,** 449–472 (1986).
7. M. Vignes-Adler, P. M. Adler and P. Gougat, Transport processes along fractals. The Cantor–Taylor brush, *PCH* **8**(4), 401–422 (1987).
8. I. Ene et E. Sanchez-Palencia, Equations et phénomènes de surface pour l'écoulement dans un modèle de milieu poreux, *J. Méc.* **14**(1), 73–108 (1975).
9. T. Levy and E. Sanchez-Palencia, On boundary conditions for fluid flow in porous media, *Int. J. Engng Sci.* **13,** 923–940 (1975).
10. J. C. Larrea, I.N.P.T. Thesis (in preparation).
11. P. Chassaing, Mélange turbulent de gaz inerte dans un jet de tube libre, Thèse Doctorat d'Etat, I.N.P.T. (1979).
12. E. Verollet, Etude d'une couche limite turbulente avec aspiration et chauffage à la paroi, Thèse d'Etat, Université de Provence (1972).
13. B. E. Launder, Turbulence models and their applications. In *Collection de la Direction des études et recherches d'Electricité de France*, Vol. 56. Edition Eyrolles (1984).
14. A. J. Grass, Structural features of turbulent flow over smooth and rough boundaries, *J. Fluid Mech.* **50,** 233 (1971).
15. S. J. Kline, The structure of turbulent boundary layers, *J. Fluid Mech.* **30,** 741 (1967).
16. T. M. Liu and J. S. Mount, Friction drag measurements of acoustic surfaces, *AIAA J.* **83,** 1356 (1983).
17. P. Crausse, Etude fondamentale des transferts couplés de chaleur et de masse en milieu poreux non-saturé, Thèse Doctorat d'Etat, I.N.P.T. (1983).
18. C. Moyne, Transferts couplés chaleur-masse lors du séchage. Prise en compte du mouvement de la phase gazeuse, Thèse d'Etat, I.N.P.L. (1987).
19. S. Bories, Recent advances in modelisation of coupled heat and mass transfer in capillary-porous bodies, *Proc. Sixth Int. Drying Symp.*, pp. KL.47–KL.61 (1988).
20. J. Philip and D. A. de Vries, Simultaneous transfer of heat and moisture in porous media, *Trans. Am. Geophys. Un.* **39,** 909–916 (1958).
21. A. V. Luikov, *Heat and Mass Transfer in Capillary Porous Bodies*. Pergamon Press, Oxford (1966).

22. S. Whitaker, Simultaneous heat, mass and momentum transfer in porous media. A theory of drying in porous media, *Adv. Heat Transfer* **13**, 119–200 (1977).
23. R. Lenormand, E. Touboul and C. Zarcone, Numerical models and experiments on immiscible displacements in porous media, *J. Fluid Mech.* **189**, 165–218 (1988).
24. J. Maneval and S. Whitaker, Effects of saturation heterogeneities on the interfacial mass transfer relation, *Proc. Sixth Int. Drying Symp.*, pp. OP.499–OP.506 (1988).
25. W. Masmoudi, Contribution à l'étude fondamentale du séchage des materiaux capillaro-poreux, Thèse I.N.P.T. (1990).
26. W. Masmoudi and M. Prat, Experimental study of the drying of porous media by means of micromodels, *Proc. Sixth Int. Drying Symp.*, pp. PB.5–PB.11 (1988).
27. T. M. Shaw, Drying as an immiscible displacement process with fluid counterflow, *Phys. Rev. Lett.* **59**(15), 1671–1674 (1987).
28. M. Suzuki and S. Maeda, On the mechanism of drying of granular beds, *J. Chem. Engng Japan* **1**, 26–31 (1968).
29. E. U. Schlunder, On the mechanism of the constant drying rate period, *Proc. Sixth Int. Drying Symp.*, pp. OP.487–OP.490 (1988).
30. M. Sifaoui et A. Perrier, Caractérisation de l'évaporation profonde, *Int. J. Heat Mass Transfer* **21**, 629–637 (1978).
31. R. Morgan and S. Yerazunis, Heat and mass transfer between an evaporative interface in a porous medium and an external gas stream, *A.I.Ch.E. Jl* **13**(1), 132–140 (1967).
32. M. Prat, Heat and mass transfers predetermination between a drying material and an external flow, *Proc. Fifth Int. Drying Symp.*, pp. 105–112 (1986).
33. W. M. Kays and M. E. Crawford, *Convective Heat and Mass Transfer*. McGraw-Hill, New York (1980).
34. M. Prat, Modélisation des transferts en milieux poreux. Changement d'échelle et conditions aux limites, Thèse Doctorat d'Etat, I.N.P.T. (1989).
35. S. Bories, G. Bacon and M. Recan, Experimental and numerical study of coupled heat and mass transfer in porous materials, *Proc. 4th Int. Drying Symp.*, pp. 159–164 (1984).
36. P. Chen and D. Pei, A mathematical model of drying processes, *Int. J. Heat Mass Transfer* **32**, 297–310 (1989).
37. B. Perrin and D. Darolles, The relation between heat and mass transfer coefficients at the contact of a porous medium on a turbulent external flow, *Proc. Sixth Int. Drying Symp.*, pp. PC37–PC41 (1988).
38. J. Van Brakel and P. M. Heertjes, On the period of constant drying rate, *Proc. 1st Int. Drying Symp.*, pp. 70–75 (1978).
39. N. Gidas and T. Constantinou, Non-dimensional numbers associated with the evaporation from a capillary porous medium, *Hydrological Sci. J.* **28**, 4, 12, 539–549 (1983).

TRANSFERTS DE CHALEUR ET DE MASSE ENTRE UN MILIEU POREUX ET UN ECOULEMENT D'AIR EXTERNE. APPLICATION AU SECHAGE DES MATERIAUX CAPILLARO-POREUX

Résumé—Une méthode numérique permettant de prédéterminer les transferts de masse et de chaleur entre un écoulement d'air externe et un corps poreux non-saturé est présentée. A partir de diverses simulations numériques, on étudie en particulier les coefficients de transferts interfaciaux de masse et de chaleur. Ces simulations montrent que les effets de bord d'attaque sont à l'origine d'une non-uniformité spatiale des gradeurs à l'interface. Il en résulte que les coefficients convectifs interfaciaux peuvent différer des valeurs standard correspondant au cas d'une couche limite sur plaque plane avec distribution uniforme de concentration ou de température à la paroi. De plus, on montre que lorsque les effets de bords d'attaque intéressent une partie suffisamment importante du corps poreux considéré, la simulation des phénomènes par un modèle monodimensionnel conduit nécessairement à des résultats incorrects. Enfin, on discute de l'influence de l'apparition en cours de séchage d'hétérogénéités macroscopiques de teneurs en eau à l'interface sur les coefficients de transfert.

WÄRME- UND STOFFÜBERGANG ZWISCHEN EINEM PORÖSEN MEDIUM UND EINER PARALLEL GERICHTETEN ÄUSSEREN STRÖMUNG—ANWENDUNG AUF TROCKNUNG KAPILLARPORÖSER MATERIALIEN

Zusammenfassung—Es wird ein numerisches Verfahren zur Berechnung des Wärme- und Stoffübergangs zwischen einem ungesättigten porösen Medium und einer äußeren Luftströmung vorgestellt. Mit verschiedenen numerischen Simulationsrechnungen wird das Verhalten der Wärme- und Stoffübergangskoeffizienten durch Konvektion an der Grenzfläche beim Trocknen untersucht. Die Rechenergebnisse zeigen, daß die Variablen an der Grenzfläche infolge der Anströmeffekte nicht konstant sind. Daraus folgt, daß die Übergangskoeffizienten an der Grenzfläche sich von Standardwerten unterscheiden, welche sich für eine Grenzschichtströmung an einer ebenen Platte mit gleichförmiger Temperatur oder Konzentrationsverteilung an der Wand ergeben. Die eindimensionale Simulation des Phänomens führt unvermeidlich zu falschen Ergebnissen, wenn der Anströmeffekt einen ausreichend großen Teil des porösen Körpers beeinflußt. Abschließend wird noch der Einfluß einer makroskopischen Ungleichverteilung des Wassergehalts an der Grenzfläche beim Trocknen untersucht.

ИССЛЕДОВАНИЕ ТЕПЛО- И МАССООБМЕНА МЕЖДУ ПОРИСТОЙ СРЕДОЙ И ПРОДОЛЬНЫМ ВНЕШНИМ ПОТОКОМ ПРИМЕНИТЕЛЬНО К СУШКЕ КАПИЛЛЯРНО-ПОРИСТОГО ВЕЩЕСТВА

Аннотация—Описывается численный метод определения тепло- и массообмена между ненасыщенной пористой средой и внешним потоком воздуха. Проводится численное моделирование с целью исследования поведения коэффициентов конвективного тепло- и массообмена на границе раздела в процессе сушки. Расчеты показывают, что эффекты передней кромки вызывают пространственную неоднородность переменных на границе раздела, вследствие чего коэффициенты межфазного переноса отличаются от стандартных значений, соответствующих течениям в пограничном слое на плоской пластине с постоянной температурой или концентрацией на стенке. Показано также, что в том случае, когда эффекты передней кромки затрагивают значительную часть пористого тела, одномерное моделирование рассматриваемых явлений приводит к некорретным результатам. Кроме того, исследуется эффект возникновения крупномасштабных неоднородностей влагосодержания на границе раздела в процессе сушки.